View metadata, citation and similar papers at core.ac.uk

brought to you by CORE

provided by Elsevier - Publisher Connector

Biophysical Journal Volume 90 January 2006 381–389

Quantification of Calcium Entry at the T-Tubules and Surface Membrane in Rat Ventricular Myocytes

F. Brette,* L. Sallé,† and C. H. Orchard*

*Department of Physiology, Medical Sciences Building, University of Bristol, Bristol, United Kingdom; and †Laboratoire de Physiologie Cellulaire, EA3212, Université de Caen, 14032 Caen, France

ABSTRACT The action potential of cardiac ventricular myocytes is characterized by its long duration, mainly due to Ca flux through L-type Ca channels. Ca entry also serves to trigger the release of Ca from the sarcoplasmic reticulum. The aim of this study was to investigate the role of cell membrane invaginations called transverse (T)-tubules in determining Ca influx and action potential duration in cardiac ventricular myocytes. We used the whole cell patch clamp technique to record electrophysiological activity in intact rat ventricular myocytes (i.e., from the T-tubules and surface sarcolemma) and in detubulated myocytes (i.e., from the surface sarcolemma only). Action potentials were significantly shorter in detubulated cells than in control cells. In contrast, resting membrane potential and action potential amplitude were similar in control and detubulated myocytes. Experiments under voltage clamp using action potential waveforms were used to quantify Ca entry via the Ca current. Ca entry after detubulation was reduced by ~60%, a value similar to the decrease in action potential duration. We calculated that Ca influx at the T-tubules is 1.3 times that at the cell surface (4.9 vs. 3.8 μmol/L cytosol, respectively) during a square voltage clamp pulse. In contrast, during a cardiac action potential, Ca entry at the T-tubules is 2.2 times that at the cell surface (3.0 vs. 1.4 μmol/L cytosol, respectively). However, more Ca entry occurs per μm^2 of junctional membrane at the cell surface than in the T-tubules (in nM/μm^2: 1.43 vs. 1.06 during a cardiac action potential). This difference is unlikely to be due to a difference in the number of Ca channels/junction at each site because we estimate that the same number of Ca channels is present at cell surface and T-tubule junctions (~35). This study provides the first evidence that the T-tubules are a key site for the regulation of action potential duration in ventricular cardiac myocytes. Our data also provide the first direct measurements of T-tubular Ca influx, which are consistent with the idea that cardiac excitation-contraction coupling largely occurs at the T-tubule dyadic clefts.

INTRODUCTION

During the cardiac action potential (AP), Ca influx via individual L-type Ca channels activates a cluster of adjacent sarcoplasmic reticulum (SR) Ca release channels (ryanodine receptors; RyRs); the consequent systolic Ca transient is the spatial and temporal sum of such local Ca releases (1,2). It is now generally accepted that L-type Ca current (I_{Ca}) is the major trigger for SR Ca release (3–5), and that alternative pathways (Na/Ca exchange, T-type Ca current) are weak triggers under physiological conditions (6,7). The rise of intracellular Ca leads to contraction of the cardiomyocyte; relaxation is brought about by Ca extrusion from the cell and resequestration into intracellular stores, via Ca ATPases and Na/Ca exchange (8). I_{Ca} also helps to load the SR with Ca for subsequent release (9): the contribution of the late phase of I_{Ca} to SR Ca loading has been demonstrated using action potential waveforms in voltage clamp experiments on guinea-pig ventricular myocytes (10), and the substantial role of I_{Ca} in SR Ca loading has been demonstrated in previous work from Eisner's laboratory (reviewed in 11). Ca is thus both a second messenger (above) and a charge carrier: I_{Ca} is a depolarizing current and therefore determines the shape of the action potential.

Although I_{Ca} is present on the sarcolemma of cardiac myocytes, it has become increasingly clear that it is not uniformly distributed on the cardiac cell membrane. The sarcolemma of mammalian ventricular myocytes contains invaginations called transverse (T)-tubules (see 12 for review). T-tubules occur perpendicularly to the longitudinal axis of the cell at intervals of ~1.8–2 μm (13,14). They are located at the Z-lines and have a mean diameter of ~250 nm (14,15). Several studies have shown that I_{Ca} is located predominantly in the T-tubules in ventricular myocytes (see 12 for review). For example, immunocytochemistry has shown that in ventricular cells staining of L-type Ca channels occurs primarily at the T-tubules in rabbit (16), guinea-pig (17), and rat (18) myocytes. These data are supported by work investigating the functional localization of I_{Ca}: we have developed a technique to disrupt the T-tubules of rat ventricular myocytes (detubulation) (19). After osmotic shock, the T-tubules seal off within the cell and hence are physically and electrically uncoupled from cell surface membrane (20). By comparing currents from detubulated and control myocytes it is possible to estimate the proportion of current within the T-tubules. We have found ~80% of I_{Ca} within the T-tubules (21). This concentration of I_{Ca} at the T-tubules (and its colocalization with RyRs) allows spatial and temporal synchronization of Ca release throughout the cell, ensuring rapid and synchronous contraction (20,22,23). Although we have previously characterized the role of I_{Ca} at the T-tubules and cell surface

Submitted June 17, 2005, and accepted for publication September 27, 2005.

Address reprint requests to Dr. Fabien Brette, Dept. of Physiology, Medical Sciences Bldg., University of Bristol, Bristol, UK. Tel.: 44-117-331-7585; Fax: 44-117-331-7585; E-mail: f.brette@bristol.ac.uk.

© 2006 by the Biophysical Society

0006-3495/06/01/381/09 $2.00

doi: 10.1529/biophysj.105.069013

in triggering SR Ca release (21), they are no quantitative data about Ca entry at the two sites. Furthermore, no information is available on the role of T-tubules in shaping the AP.

In this study, we have therefore investigated the role of the T-tubules in determining action potential configuration. We have also examined Ca entry in control and detubulated myocytes under voltage clamp using square and action potential waveforms, to quantify Ca entry at the T-tubule and surface membranes.

MATERIALS AND METHODS

Isolation of rat ventricular myocytes

Male Wistar rats (250–300 g) were killed humanely by cervical dislocation after stunning, and the heart rapidly removed, in accordance with the United Kingdom Home Office Guidance on the Operation of the Animals (Scientific Procedures) Act of 1986. The heart was mounted on a Langendorff apparatus and perfused retrogradely with a HEPES-based isolation solution containing (in mmol/L): 130 NaCl, 5.4 KCl, 0.4 NaH_2PO4, 1.4 $MgCl_2$, 0.75 $CaCl_2$, 10 HEPES, 10 glucose, 20 taurine, and 10 creatine (pH 7.3 with NaOH). When the coronary circulation had cleared of blood, perfusion was continued with Ca-free isolation solution (in which $CaCl_2$ was replaced with 0.1 mmol/L EGTA) for 5 min, followed by perfusion for a further 7–10 min with isolation solution containing 0.8 mg/ml collagenase (type I; Worthington Biochemical, Lakewood, NJ), and 0.08 mg/ml protease (type XIV; Sigma, St. Louis, MO). The ventricles were then excised from the heart, minced, and gently shaken at 37°C in collagenase-containing isolation solution supplemented with 1% bovine serum albumin. Cells were filtered from this solution at 5 min intervals and resuspended in isolation solution containing 0.75 mmol/L Ca.

Detubulation of rat ventricular myocytes

Detubulation was induced by osmotic shock as described previously (19). Briefly, 1.5 mol/L formamide was added to the cell suspension for 15–20 min, before returning the cells to the standard solution. Detubulation occurs because of the osmotic shock produced by formamide withdrawal.

Electrophysiological recordings

Myocytes were studied in a chamber mounted on the stage of an inverted microscope (Nikon Diaphot, Tokyo, Japan). Cells were initially superfused with a normal physiological salt solution containing (in mmol/L): 113 NaCl, 5 KCl, 1 MgSO4, 1 $CaCl_2$, 1 Na_2HPO_4, 20 Na acetate, 10 glucose, 10 HEPES, and 5 U/L insulin, pH set to 7.4 with NaOH. All experiments were performed at room temperature (22–25°C).

Membrane potential and currents were recorded using the whole-cell configuration of the patch clamp technique (24). An Axopatch 200B (Axon Instruments, Union City, CA) amplifier was used, controlled by a Pentium PC connected via a Digidata 1322A A/D converter (Axon Instruments), which was also used for data acquisition and analysis using pClamp software (Axon Instruments). Signals were filtered at 2–10 kHz using an 8-pole Bessel low pass filter before digitization at 10–20 kHz and storage. Patch pipettes resistance was typically 1.5–2.5 MΩ when filled with intracellular solution (below).

Action potentials were evoked by 2.5 ms subthreshold current steps. Trains of pulses were applied at 0.1 Hz. The bath solution was the normal physiological salt solution described above. The pipette solution contained (in mmol/L): 130 K-glutamate, 9 KCl, 10 NaCl, 0.5 $MgCl_2$, 5 Mg-ATP, 0.5 EGTA, 10 HEPES, 0.4 GTPTris, set to pH 7.2 with CsOH.

I_{Ca} was measured using Na- and K-free external and internal solutions to avoid contamination by overlapping ionic currents, and to allow us to use a physiological holding potential (21). The external solution contained (in mmol/L): 5 4AP, 130 TEACl, 0.5 $MgCl_2$, 10 HEPES, 10 Glucose, 1 $CaCl_2$, pH set to 7.4 using TEAOH. The pipette solution contained (in mmol/L): 110 CsCl, 20 TEACl, 0.5 $MgCl_2$, 5 Mg-ATP, 5 EGTA, 10 HEPES, 0.4 GTPTris, set to pH 7.2 with CsOH. At least 5 min was allowed for cell dialysis by the pipette solution before experiments were initiated. Cell membrane capacitance was measured by integrating the capacitance current recorded during a 10-mV hyperpolarizing pulse from −80 mV. Cell capacitance and series resistance were compensated (> 80%) so that the maximum voltage error was <3.5 mV. I_{Ca} was elicited by either a rectangular step (150-ms pulse to 0 mV from a holding potential of −80 mV) or a representative action potential waveform. The action potential waveforms were the average of the APs recorded in the current clamp experiments in control and detubulated myocytes ($n = 10$ of each cell type, see Fig. 1 *A*). Trains of depolarizing pulses were applied at 0.1 Hz.

Data analysis

Action potential amplitude was measured as the difference between the overshoot and the resting membrane potential. Membrane potentials were corrected by −11 mV to compensate for liquid junction potentials between the external and pipette solutions. APD was measured as the duration from the overshoot to three different percentages of repolarization (25: APD_{25}; 50: APD_{50}; 90: APD_{90}).

I_{Ca} was measured as the difference between the peak inward current and the current at the end of the depolarizing pulse. Currents are expressed as current density (pA/pF). Time to peak I_{Ca} was measured from the start of the depolarizing pulse. Because the decay of I_{Ca} varied between cell types and experimental conditions, the kinetics of inactivation of I_{Ca} were characterized by the time required for the current to decay to 0.37 of the peak amplitude ($T_{0.37}$) (21). I_{Ca} was also analyzed by integrating I_{Ca} during the test pulse to obtain total Ca influx during the pulse. Ca entry is expressed as charge density (fC/pF) and as cytosolic [Ca] using estimates of surface to volume ratios for control and detubulated cardiac myocytes (25).

Chemicals

All solutions were prepared using ultrapure water supplied by a Milli-Q system (Millipore, Watford, UK). All solution constituents were reagent grade and purchased from Sigma (St. Louis, MO).

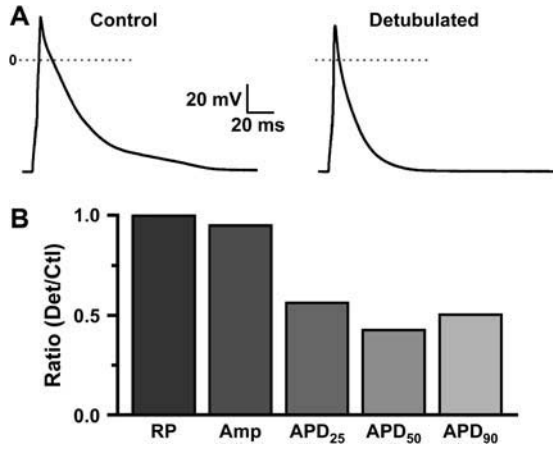

FIGURE 1 Action potentials are shorter after detubulation. (*A*) Mean action potential obtained in 10 control (*left*) and 10 detubulated (*right*) rat ventricular myocytes. (*B*) The mean ratio between resting potential (RP), action potential amplitude (Amp), APD_{25}, APD_{50}, and APD_{90} in detubulated and control myocytes.

Statistics

Data are presented as mean ± SE. Statistical analysis was performed using SigmaStat software. A two-tailed unpaired *t*-test was used to compare data from control and formamide treated cells, after confirmation of normal distribution and equal variance. Friedman Repeated Measures Analysis of Variance on Ranks and Student-Newman-Keuls Method were used to test the effect of multiple voltage waveforms within the same group of cells. $P < 0.05$ was taken as significant.

RESULTS

Detubulation shortens the action potential

Fig. 1 *A* shows action potentials elicited by brief current pulses at 0.1 Hz in control and detubulated ventricular myocytes. Each trace shows the mean of the APs recorded from 10 control (*left*) and 10 detubulated (*right*) myocytes; these mean APs were used as representative action potentials for subsequent voltage clamp studies. The principal effect of detubulation was to shorten the action potential, shown by a significant reduction of APD_{25}, APD_{50}, and APD_{90} (Table 1). In contrast, resting membrane potential and action potential amplitude were unchanged (−81.2 ± 0.9 mV vs. −81.0 ± 1.2 mV; NS, and 114 ± 4 mV vs. 108 ± 3 mV; NS; $n =$ 10 myocytes of each type, Table 1). Fig. 1 *B* shows the detubulated/control ratios for these variables, showing that the effect of detubulation appears most marked for APD_{50}, the point at which I_{Ca} contributes most to the action potential (26). To investigate this further, we recorded I_{Ca} using action potential waveforms in voltage clamp experiments on control and detubulated myocytes.

I_{Ca} elicited by voltage clamp using square and action potential waveforms

I_{Ca} was elicited at 0.1 Hz in each cell type using three different voltage command waveforms: a square pulse, the control action potential, and the detubulated action potential (Fig. 2, *top panel*).

Typical results for control myocytes are shown in the middle panel of Fig. 2. Peak I_{Ca} was slightly, but significantly, smaller when the control AP waveform was used, compared to the square pulse and detubulated AP waveform (Fig. 3 *A*). However the major effects were on I_{Ca} kinetics:

TABLE 1 Action potential characteristics of control and detubulated myocytes

	Controls	Detubulated
Resting potential (mV)	−81.2 ± 0.9	−81.0 ± 1.2
Amplitude (mV)	114 ± 4	108 ± 3
APD_{25} (ms)	11.9 ± 2.1	6.7 ± 0.9*
APD_{50} (ms)	31.6 ± 5.8	13.5 ± 1.7*
APD_{90} (ms)	61.0 ± 9.8	30.7 ± 3.4*

Values are mean ± SE from 10 cells in each type; APD, action potential duration.
*$P < 0.05$.

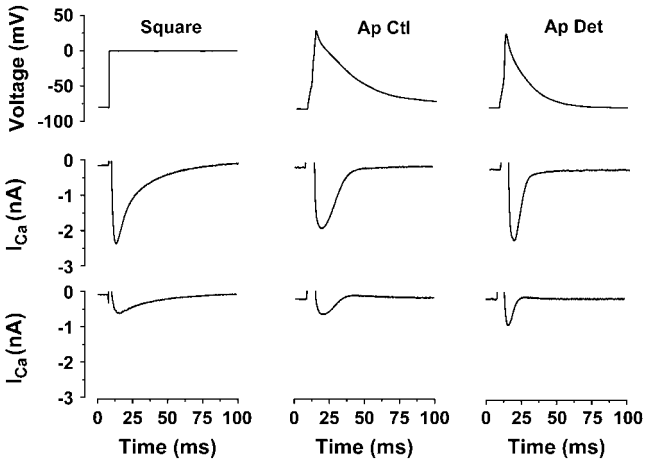

FIGURE 2 I_{Ca} during a square pulse, control AP waveform and detubulated waveform in control and detubulated myocytes. The top panel shows the voltage waveform applied to cardiac myocytes (square pulse, *left*; control action potential, *middle*; detubulated action potential, *right*). The middle panel shows representative example of I_{Ca} measured in the same control rat ventricular myocyte under the conditions shown directly above (cell capacitance, 210 pF). The lower panel shows representative example of I_{Ca} measured in the same detubulated rat ventricular myocyte under the conditions shown on the top panel (cell capacitance, 110 pF).

time to peak I_{Ca} was significantly longer when using AP waveforms, compared to the square pulse, and this was more marked for control than detubulated AP waveforms (13.8 ± 1 ms vs. 10.9 ± 0.2 ms, $n = 12$, $P < 0.05$, Fig. 3 *B*). Part of the longer time to peak can be explained by the longer time to maximum depolarization when using AP waveforms (indicated by the longer capacitance transients, see Fig. 2). The kinetics of inactivation were also markedly different: during the square pulse, the decay of I_{Ca} was biphasic because of fast Ca-dependent inactivation and slower voltage dependent inactivation (27). However biphasic inactivation was absent when using AP waveforms. Inactivation (monitored as $T_{0.37}$, see Methods) was also slightly faster when using control AP waveform compared to square pulse and significantly faster when using detubulated AP waveform (Fig. 3 *C*).

The lower panel of Fig. 2 shows typical results for a detubulated myocyte. Detubulation resulted in a significant decrease in cell capacitance (by 28.5%; 186 ± 11 pF in 14 control cells vs. 133 ± 8 pF in 13 detubulated cells, $P <$ 0.05). Peak I_{Ca} also decreased, because I_{Ca} is concentrated at the T-tubules, consistent with previous work (21): peak I_{Ca} density was significantly smaller than control myocytes for all voltage waveforms (Fig. 3 *A*). In contrast, the time to peak was not significantly different from control myocytes (Fig. 3 *B*). $T_{0.37}$ was longer than in control myocytes when using a square pulse (Fig. 3 *C*), as described previously (21) but surprisingly, $T_{0.37}$ was similar in control and detubulated myocytes when using the AP waveforms (Fig. 3 *C*). These data show that a large proportion of Ca influx occurs across the T-tubule membrane, and that Ca influx depends on the

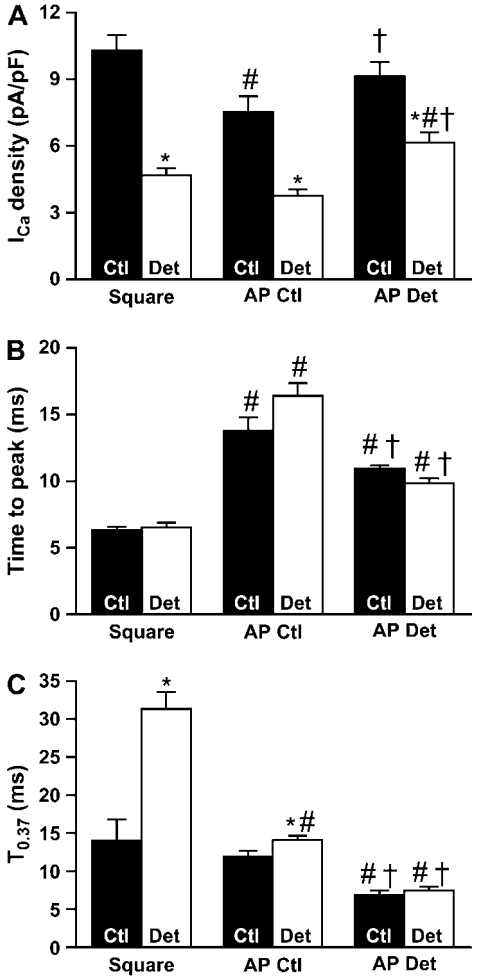

FIGURE 3 I_{Ca} characteristics during square pulse, control AP waveform, and detubulated waveform in control and detubulated myocytes. (*A*) Mean (± SE) I_{Ca} density in control (*solid bars*) and detubulated (*open bars*) rat ventricular myocytes during square pulse (*Square*, *left*), control AP waveform (*AP Ctl*, *middle*), and detubulated AP waveform (*AP Det*, *right*). (*B*) Mean (± SE) time to peak I_{Ca} in control (*solid bars*) and detubulated (*open bars*) rat ventricular myocytes during square pulse (*Square*, *left*), control AP waveform (*AP Ctl*, *middle*), and detubulated AP waveform (*AP Det*, *right*). (*C*) Mean (± SE) time to decline to 37% of peak I_{Ca} ($T_{0.37}$) in control (*solid bars*) and detubulated (*open bars*) rat ventricular myocytes during square pulse (*Square*, *left*), control AP waveform (*AP Ctl*, *middle*), and detubulated AP waveform (*AP Det*, *right*). Data are from 12 control and 13 detubulated myocytes. $^{*}P < 0.05$ between cell types, $^{\#}P < 0.05$ versus square pulse, and $^{\dagger}P < 0.05$ versus AP Ctl.

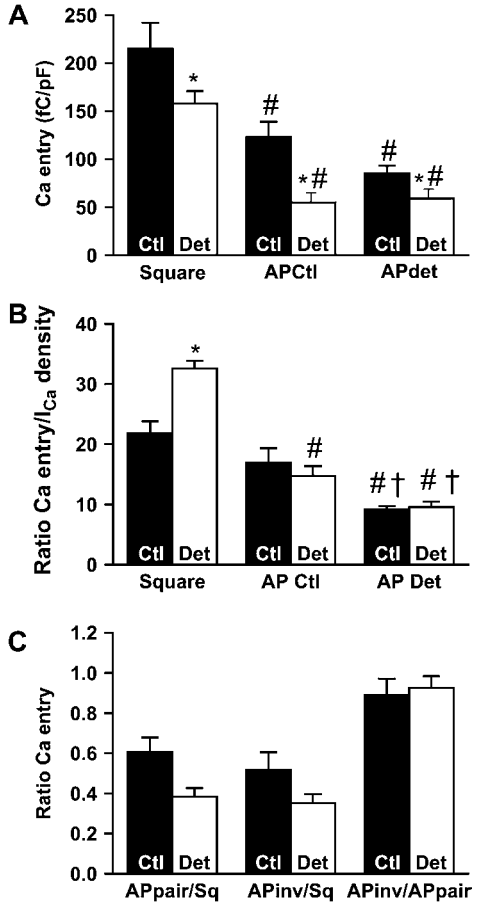

FIGURE 4 Ca entry during I_{Ca} is smaller after detubulation. (*A*) Mean (± SE) Ca entry during I_{Ca} in control (*solid bars*) and detubulated (*open bars*) rat ventricular myocytes during square pulse (*Square*, *left*), control AP waveform (*AP Ctl*, *middle*), and detubulated AP waveform (*AP Det*, *right*). (*B*) Ratio Ca entry/peak I_{Ca} for control (*solid bars*) and detubulated (*open bars*) rat ventricular myocytes during square pulse (*Square*, *left*), control AP waveform (*AP Ctl*, *middle*), and detubulated AP waveform (*AP Det*, *right*). (*C*) Mean (± SE) ratio for control (*solid bars*) and detubulated (*open bars*) myocytes when cells are stimulated with AP of their own type (APpair) and the other type (APinv). Data are from 12 control and 13 detubulated myocytes. $^{*}P < 0.05$ between cell types, $^{\#}P < 0.05$ versus square pulse, and $^{\dagger}P < 0.05$ versus AP Ctl.

voltage waveform used; these data were used, therefore, to quantify Ca entry across the T-tubule and surface membranes when using different waveforms.

Ca entry during voltage clamp using action potential waveforms

I_{Ca} was integrated, and the integral normalized to cell capacitance, to quantify Ca entry. Fig. 4 *A* shows that Ca influx was significantly smaller in detubulated cells than in control cells when using a given waveform, but was larger during square pulse stimulation, compared to AP waveforms, in both cell types. Fig. 4 *B* shows the ratio of Ca entry/peak I_{Ca} density, showing that a given peak I_{Ca} produced more Ca influx in detubulated myocytes than in control myocytes during a square pulse, but that this difference was absent when using AP waveforms. The ratio of net entry of positive charge when using the detubulated AP for detubulated myocytes versus control AP for a control myocyte was 0.421 (8.3 ± 1.4 pC vs. 23.5 ± 4.2 pC, $n = 13$ and 12, respectively). This is similar to the ratio of APD_{50} for detubulated versus control myocytes (0.427, Fig. 1 *B*). Thus the reduction in Ca entry after detubulation is compatible with the reduction in APD shown in Fig. 1, and with the idea

that the role of the T-tubules in shaping AP configuration is mainly due to the localization of I_{Ca} is these invaginations. Conversely, AP waveform can influence $I_{Ca,}$ and therefore Ca entry. We examined this by calculating the ratio of Ca entry during different voltage waveforms (Fig. 4 *C*). The ratio of Ca entry is reduced when using AP waveforms (either control or detubulated) compared to square pulse, although AP voltage waveform (control versus detubulated) has little effect upon Ca entry in either cell type, as the ratio is ~1 (Fig. 4 *C*, *right*). This suggests that reduction of APD has little effect upon Ca entry via I_{Ca}, therefore the decrease in Ca entry after detubulation is mainly due to a decrease in I_{Ca} rather than a decrease in APD.

Quantification of Ca entry at the surface membrane and T-tubules

The main findings of this study are summarized in Table 2. Ca fluxes and I_{Ca} in the T-tubules were calculated as the difference in whole-cell Ca entry between control and detubulated myocytes. These Ca fluxes and I_{Ca} were divided by the difference in membrane capacitance between control and detubulated cells, to derive the Ca flux and I_{Ca} density in the T-tubules. The data from detubulated myocytes have been corrected by 10% to account for the presence of nondetubulated myocytes (25).

In rat ventricular myocytes, Ca entry is greater when using the square voltage waveform than when using the AP waveform (Table 2). Ca entry at the T-tubules represents 53% and 65% of total during a square pulse and AP waveform, respectively. These values are less than the percentage of I_{Ca} at the T-tubules (75%).

These Ca influx measurements were further converted to changes in [Ca]. Integrated fluxes were converted to molar quantity (by dividing by zF) and normalized to cell volume. Surface/volume ratios (5.1 and 3.4 pF/pL in control and detubulated myocytes from our recent study (25)) give a volume of 36.4 ± 2.2 pL for control ($n = 14$) and 39.22 ± 2.3 pL for detubulated myocytes ($n = 13$); these values are not significantly different. Fig. 5 shows the results of these

TABLE 2 Distribution of mean cell capacitance, I_{Ca}, and Ca entry in the external sarcolemma and T-tubules

	Surface area (pF)	I_{Ca} SP (pA/pF)	Ca entry SP (fC/pF)	Ca entry AP (fC/pF)
Total SL (control cells)	186	10.3	215	108
External SL (detubulated cells)*	127	3.8	149	55
T-tubules (calculated)	59	24.3	357	222
% in T-tubules	32	75	53	65
Density T-tub/ext SL		6.4	2.4	4

SP, square pulse; AP, action potential; SL, sarcolemma.
*These values have corrected by 10% for the presence of nondetubulated myocytes.

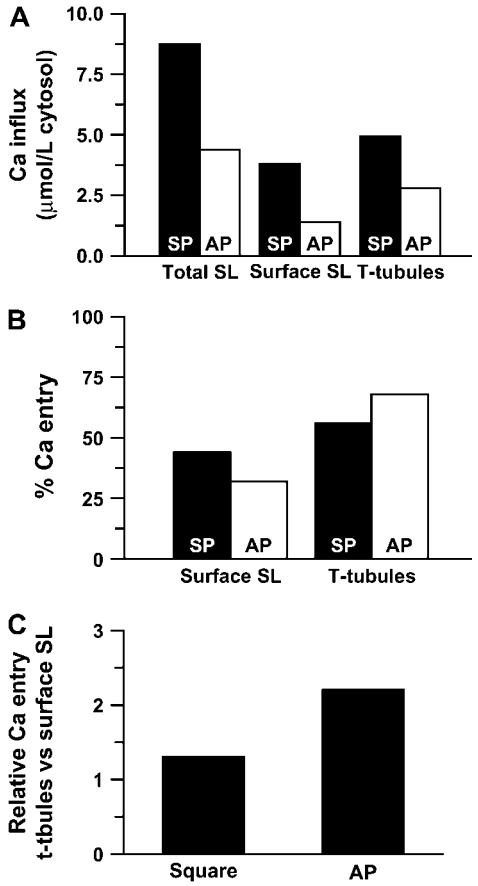

FIGURE 5 Relative distribution of Ca entry between the T-tubules and external sarcolemma. (*A*) Mean Ca entry during square pulse (*solid bars*) and AP waveform (*open bars*) at the total sarcolemma (*Total SL*, *left*), surface sarcolemma (*Surface SL*, *middle*), and T-tubules (*right*) during action potential stimulation. Ca fluxes are converted to $[Ca^{2+}]$ in μmol/L cytosol (see text for details). (*B*) The relative distribution of Ca entry during square pulse (*solid bars*) and AP waveform (*open bars*) at the surface sarcolemma (*Surface SL*, *left*) and the T-tubules (*right*). (*C*) The ratio between the Ca entry at surface sarcolemma and in the T-tubules during square pulse (*Square*, *left*) and AP waveform (*AP*, *right*).

calculations with [Ca] in μmol/L cytosol (assuming the fraction of nonmitochondrial cell volume to be 0.65 L cytosol/L cell (28)). Ca influx at the T-tubules is 1.3 times that at the cell surface (4.9 vs. 3.8 μmol/L cytosol, respectively) during a square pulse. In contrast, during an AP, Ca entry at the T-tubules is 2.2 times that at the cell surface (3.0 vs. 1.4 μmol/L cytosol, respectively, calculated by the difference between average of control and detubulated AP; Fig. 5, *A–C*). The percentage of Ca influx at the T-tubules is also smaller that the percentage of I_{Ca} density (Table 2).

We also estimated the junctional Ca flux at the two sites. In rat ventricular myocytes, 7.7% of the surface sarcolemma, and 48% of the T-tubules, is junctional (29). Assuming that 1 μF represents 1 cm^2 (30), we calculated that junctions represent 978 μm^2 at the cell surface and 2832 μm^2 in the T-tubules (Table 3). Thus Ca influx per μm^2 of junction is 2.2 higher at the cell surface than in the T-tubules (3.89 vs.

TABLE 3 Junctional Ca entry at the surface sarcolemma and T-tubules

	External SL	T-tubules
Total surface area (pF)	127	59
Junctional surface area (μm^2)*	978	2832
Ca entry SP (μM)	3.8	4.9
Ca entry AP (μM)	1.4	3.0
Ca entry per μm^2 junction (nM) SP	3.89	1.73
Ca entry per μm^2 junction (nM) AP	1.43	1.06

SP, square pulse; AP, action potential; SL, sarcolemma.
*These values have been calculated assuming that junctional sarcolemma forms 7.7% of the surface SL and 48% of the t-tubule membrane (29).

1.73 nmol/L cytosol/μm^2, respectively) during a square pulse, and 1.3 times higher during an AP (1.43 vs. 1.06 nmol/L cytosol/μm^2, respectively; Table 3). To investigate whether the greater Ca entry per μm^2 of cell surface, compared to the T-tubules, is due to a difference in the number of Ca channels at each junction, we estimated the total number of Ca channels, using the equation $N = I_{Ca}/(i_{Ca} \times p)$, where N is the number of functional channels, I_{Ca} is the whole cell Ca current (data from Table 2 converted to pA), i_{Ca} is the unitary current (0.2 pA, see Discussion), and p is the probability of channel opening (0.05, see Discussion). From these values, we estimate that 191,600 functional Ca channels are present in rat myocytes, with 48,200 channels at the cell surface and 143,400 at the T-tubules (Table 4). Expressed as Ca channel density, this gives 10.3, 3.8, and 24.3 Ca channels/μm^2 at the total sarcolemma, cell surface, and T-tubules, respectively. These values are in the range observed by others in cardiac preparations (see 31 and 32 for review). We next estimated the number of junctions in the myocyte. Data from electron microscopy have shown that in rat ventricular myocytes a typical junction consists of 267 feet (ryanodine receptors), each separated by 29 nm, with a minimum distance between junctions of 414 nm (33); this give a minimum mean area of 0.788 μm^2 for each junction plus its surrounding membrane. This enables us to calculate the (maximum) total number of junctions as 4832, and hence, from junctional surface area at the two sites (Table 3) that 1240 junctions are present at the cell surface and 3592 at the T-tubules (Table 4). Given that 90% of Ca channels are junctional (18), we estimate that a typical junction in rat ventricular myocytes contains ~35 Ca channels at both the cell surface and T-tubules (Table 4).

TABLE 4 Number of Ca channels per junction at the surface sarcolemma and T-tubules

	Total SL	External SL	T-tubules
Number of Ca channels*	191,600	48,200	143,400
Number of junctions†	4832	1240	3592
Ca channels per junction‡	35.7	35.0	35.9

SL, sarcolemma.
*These values have been calculated assuming that at 0 mV, the unitary current is 0.2 pA and probability of channel opening is 0.05 (see text for details).
†These values have been calculated assuming that a typical rat junction is formed by 267 ryanodine receptors and the minimum distance between junctions is 414 nm (33).
‡These values have been calculated assuming that 90% of Ca channels are junctional (18).

DISCUSSION

This study provides the first quantitative description of Ca entry at the T-tubules and cell surface of cardiac ventricular myocytes.

Experimental approach

The method used to detubulate rat ventricular myocytes has been described and validated previously (19,20). Notably, this procedure has no effect on cell capacitance, I_{Ca} or the AP in atrial myocytes, which lack T-tubules (20). This method enables investigation of the physiological function of surface and T-tubule membranes in rat ventricular myocytes. Using this technique, we have shown previously that L-type Ca current, Na/Ca exchange and Na-K pump currents are located predominantly in the T-tubules (21,25). In contrast, K currents are evenly distributed between the surface sarcolemma and T-tubules (34). We have also shown that the T-tubules are essential for spatial and temporal synchronization of Ca release throughout the cell (20,23,35).

We chose to use Na- and K-free experimental solutions to record I_{Ca} because this enabled us to use a physiological resting potential (near −80 mV for step and AP waveforms) without contamination by other currents, such as Na current, Na/Ca exchanger current, and K currents, allowing us to quantify Ca entry via I_{Ca} only. The use of a physiological holding potential is important since depolarized holding potentials (e.g., −40 mV) are closer to the activation threshold of I_{Ca} and can therefore interfere with Ca channel availability and gating (see 32 for review). However, we might have slightly underestimated Ca entry because of the lack of Na/Ca exchange activity, although Ca entry via this route in cardiac myocytes is small compared to I_{Ca} (8). Inclusion of a low concentration of a slow Ca buffer (5 mmol/L EGTA) in the pipette solution allows Ca in the bulk cytosol to be ''clamped'' (indicated by the absence of cell contraction) while permitting Ca in the dyadic space to change (27). Therefore, Ca entry via I_{Ca} measured in this study is close to Ca entry during normal excitation-contraction coupling.

Role of the T-tubules in action potential shape

The main effect of loss of the T-tubules was to decrease APD. This shortening is unlikely to be due to differences in K currents because they are evenly distributed between surface membrane and T-tubules (34), consistent with the absence of changes in the resting membrane potential

(mainly due to I_{K1} in cardiac myocytes, 31). Reduction of APD is also unlikely to be due to a change in Na current because: i), Na current causes only a small entry of positive charge because it is very brief (36); and ii), AP amplitude, which is mainly due to Na current, is the same in control and detubulated myocytes, compatible with uniform distribution of Na current at the cell surface (23). It is therefore more likely that the decrease in APD is due to less I_{Ca} and Na/Ca exchange current, which carry positive charge into the cell and are concentrated at the T-tubules (21,25). Given the results from this study, it is expected that the AP in the T-tubules of cardiac myocytes will be longer than at the cell surface. Calculation from APD_{50} in detubulated (surface membrane) and control (total membrane) myocytes gives a value of 73.8 ms for APD_{50} in the T-tubules (30% of membrane), ~5.5 times longer than at the cell surface. This challenging speculation of course requires experimental confirmation, but to date no electrophysiological technique has enabled recording of electrical activity of the T-tubules only. The action potential is shaped by ionic currents; conversely the form of the action potential influences ionic currents. This study shows that a shorter action potential enhances the magnitude and reduces the time to peak and $T_{0.37}$ of I_{Ca} (Fig. 3). This is similar to previous work showing that rapid early repolarization of the AP is crucial in shaping I_{Ca} (37,38).

Ca entry at the T-tubules versus cell surface membrane

Our data show that Ca entry during a square pulse is larger than during an AP waveform (Fig. 4). This is consistent with a previous report in rat ventricular myocytes using a similar approach (39), and highlights the caution required when interpreting results obtained using square pulses to calculate Ca flux. Our calculated Ca entry is similar to previous work using an AP waveform in rat myocytes (~120 fC/pF (40); ~4 μmol/L cytosol (41)). In contrast, Yuan et al. (39) found values that are somewhat higher than observed in this study (~14 μmol/L cytosol), but this may be due to higher external [Ca] and lower Ca-dependent inactivation. It is unlikely that the temperature used to perform our experiments (room temperature) altered the quantification of Ca entry because temperature (25°C vs. 35°C) has been shown to alter I_{Ca} kinetics but not total I_{Ca} flux in rabbit ventricular myocytes (42).

We found that Ca entry at the T-tubules is larger than at surface sarcolemma, although not to the extent of I_{Ca} density (~75%). This can be explained by reduced Ca-dependent inactivation of the Ca channels present at the cell surface (21), which will prolong I_{Ca}. However, this difference in Ca-dependent inactivation of I_{Ca} at the T-tubules and cell surface was less marked during the AP waveform (Fig. 3 *C*).

Interestingly, Ca entry after detubulation is reduced by ~60%, a value close to the density of Na/Ca exchanger present in the T-tubules (63%, (25)). Since Ca entry via I_{Ca} is extruded by the Na^+/Ca^{2+} exchanger during a normal Ca cycle in cardiac myocyte (11), this can explain how SR Ca^{2+} load remains constant after detubulation (19,23,35). The relative difference between I_{Ca} density and Ca entry at the T-tubule and surface membranes (Table 2) also suggests a different role for I_{Ca} at the two sites: the large, rapidly inactivating I_{Ca} in the T-tubules will form an effective trigger for SR Ca release (9), whereas the more slowly inactivating I_{Ca}, and relatively large Ca entry (for the density of I_{Ca}) at the cell surface will be effective in loading the SR with Ca^{2+} that can be released in response to a subsequent stimulus (9,43).

This work suggests that Ca entry per μm^2 of junctional membrane is greater at the cell surface than in the T-tubules (Table 3). When normalized to the number of junctions present (Table 4), calculated from available electron microscopy data (33), the data suggest that Ca entry is 1.13 nmol/L cytosol/junction at the cell surface versus 0.85 nmol/L cytosol/junction at the T-tubules during an action potential. However our calculation of the number of junctions may be overestimated because, to the best of our knowledge, there is currently no information about the mean distance between junctions but only the minimum distance between them (33). Similarly, our calculation of the number of Ca channels is speculative, since it depends critically on i_{Ca} (the unitary current) and p (the probability of channel opening). Experimental values are quite disparate, ranging from 0.15 to 0.4 pA for i_{Ca} and 0.015 to 0.08 for p (at 0 mV, e.g., see (44–48) and for review (31)); this probably reflects differences in species and experimental conditions between studies. We have therefore used midrange values which are classically used for computer modeling of cardiac excitation-contraction coupling ($i_{Ca} = 0.2$ pA and $p = 0.05$, see 49,50). These values give us a total Ca channel number (Table 4) that is within the range observed experimentally by others (from 28,000 (48) to 300,000 (47)). It is also important to note that we used similar parameters for cell surface and T-tubule Ca channels and this might not be the case, although no experimental data from single Ca channel recording at the T-tubules are available. We estimated that ~35 Ca channels are present at each junction in rat ventricular myocytes (independent of the subcellular location of the junction). This is somewhat higher than described by Bers (10–25 Ca channels, (31)), although rat ventricular myocytes tend to have more feet (or ryanodine receptors, 267 (33)) per junction than other species (e.g., 60 in dog, 128 in mouse; see 33). Thus our values give a ryanodine receptor/Ca channel ratio of ~7, which is in the range of other species (4–10; see 31). These considerations therefore suggest that a similar number of Ca channels are present at each junction at the cell surface and T-tubules. Thus it appears likely that greater Ca entry/Ca channel at the cell surface, rather than a greater number of Ca channels, accounts for the differential Ca influx at the two sites (Table 3).

This differential Ca entry might also have implications for the gain of SR Ca release; however previous work has

suggested that the gain of SR Ca release is similar at the surface and T-tubule membranes (21), so that the different Ca dependent inactivation at the two sites (above) is unlikely to be due to differences in local Ca release. The extensive T-tubule system therefore allows synchronous Ca release within the cell (see above). Ca entry at the cell surface provides Ca^{2+} for the SR which can then diffuse within the SR to be available for subsequent release at the T-tubules. This requires further investigation, although it has been recently shown that Ca diffuses very quickly within the SR (51,52). Such balance between Ca entry at the cell surface and T-tubules might also be important during development and in pathological conditions in which T-tubule density changes (see 12 for review); it has, for example, been reported to decrease during heart failure (53–55).

In conclusion, our study provides the first evidence that the T-tubules are a key site for the regulation of action potential duration in ventricular cardiac myocytes. Our data also provide the first direct measurements of T-tubular Ca influx, which are consistent with the idea that cardiac excitation-contraction coupling largely takes place at the T-tubule dyadic clefts. The quantification of local Ca entry within the T-tubules and at junctional membrane may also have important implications for modeling cardiac cell function and for understanding cellular Ca cycling and suggests that the key role of Ca entry may be different at the T-tubule and surface membranes.

This work was supported by The Wellcome Trust. F.B. is a Wellcome Trust fellow.

REFERENCES

1. Wang, S. Q., L. S. Song, E. G. Lakatta, and H. Cheng. 2001. Ca^{2+} signalling between single L-type Ca^{2+} channels and ryanodine receptors in heart cells. *Nature*. 410:592–596.
2. Wier, W. G., and C. W. Balke. 1999. Ca^{2+} release mechanisms, Ca^{2+} sparks, and local control of excitation-contraction coupling in normal heart muscle. *Circ. Res.* 85:770–776.
3. Beuckelmann, D. J., and W. G. Wier. 1988. Mechanism of release of calcium from sarcoplasmic reticulum of guinea-pig cardiac cells. *J. Physiol.* 405:233–255.
4. Callewaert, G., L. Cleemann, and M. Morad. 1988. Epinephrine enhances Ca^{2+} current-regulated Ca^{2+} release and Ca^{2+} reuptake in rat ventricular myocytes. *Proc. Natl. Acad. Sci. USA*. 85:2009–2013.
5. Cannell, M. B., J. R. Berlin, and W. J. Lederer. 1987. Effect of membrane potential changes on the calcium transient in single rat cardiac muscle cells. *Science*. 238:1419–1423.
6. Sipido, K. R., M. Maes, and W. F. Van De. 1997. Low efficiency of Ca^{2+} entry through the Na^{+}-Ca^{2+} exchanger as trigger for Ca^{2+} release from the sarcoplasmic reticulum. A comparison between L-type Ca^{2+} current and reverse-mode Na^{+}-Ca^{2+} exchange. *Circ. Res.* 81: 1034–1044.
7. Sipido, K. R., E. Carmeliet, and W. F. Van De. 1998. T-type Ca^{2+} current as a trigger for Ca^{2+} release from the sarcoplasmic reticulum in guinea-pig ventricular myocytes. *J. Physiol (Lond).* 508 (Pt. 2):439–451.
8. Bers, D. M. 2002. Cardiac excitation-contraction coupling. *Nature*. 415:198–205.
9. Fabiato, A. 1985. Simulated calcium current can both cause calcium loading in and trigger calcium release from the sarcoplasmic reticulum of a skinned canine cardiac Purkinje cell. *J. Gen. Physiol.* 85:291–320.
10. Linz, K. W., and R. Meyer. 1998. The late component of L-type calcium current during guinea-pig cardiac action potentials and its contribution to contraction. *Pflugers Arch.* 436:679–688.
11. Eisner, D. A., H. S. Choi, M. E. Diaz, S. C. O'Neill, and A. W. Trafford. 2000. Integrative analysis of calcium cycling in cardiac muscle. *Circ. Res.* 87:1087–1094.
12. Brette, F., and C. Orchard. 2003. T-tubule function in mammalian cardiac myocytes. *Circ. Res.* 92:1182–1192.
13. Page, E. 1978. Quantitative ultrastructural analysis in cardiac membrane physiology. *Am. J. Physiol.* 235:C147–C158.
14. Sommer, J. R., and R. B. Jennings. 1992. Ultrastructure of cardiac muscle. *In* The Heart and Cardiovascular System, Vol. 1. H. A. Fozzard, E. Haber, R. B. Jennings, A. M. Katz, and H. E. Morgan, editors. Raven Press, New York. 3–50.
15. Soeller, C., and M. B. Cannell. 1999. Examination of the transverse tubular system in living cardiac rat myocytes by 2-photon microscopy and digital image-processing techniques. *Circ. Res.* 84:266–275.
16. Carl, S. L., K. Felix, A. H. Caswell, N. R. Brandt, W. J. Ball, Jr., P. L. Vaghy, G. Meissner, and D. G. Ferguson. 1995. Immunolocalization of sarcolemmal dihydropyridine receptor and sarcoplasmic reticular triadin and ryanodine receptor in rabbit ventricle and atrium. *J. Cell Biol.* 129:672–682.
17. Gathercole, D. V., D. J. Colling, J. N. Skepper, Y. Takagishi, A. J. Levi, and N. J. Severs. 2000. Immunogold-labeled L-type calcium channels are clustered in the surface plasma membrane overlying junctional sarcoplasmic reticulum in guinea-pig myocytes-implications for excitation-contraction coupling in cardiac muscle. *J. Mol. Cell. Cardiol.* 32:1981–1994.
18. Scriven, D. R., P. Dan, and E. D. Moore. 2000. Distribution of proteins implicated in excitation-contraction coupling in rat ventricular myocytes. *Biophys. J.* 79:2682–2691.
19. Kawai, M., M. Hussain, and C. H. Orchard. 1999. Excitation-contraction coupling in rat ventricular myocytes after formamide-induced detubulation. *Am. J. Physiol.* 277:H603–H609.
20. Brette, F., K. Komukai, and C. H. Orchard. 2002. Validation of formamide as a detubulation agent in isolated rat cardiac cells. *Am. J. Physiol.* 283:H1720–H1728.
21. Brette, F., L. Salle, and C. H. Orchard. 2004. Differential modulation of L-type Ca^{2+} current by SR Ca^{2+} release at the T-tubules and surface membrane of rat ventricular myocytes. *Circ. Res.* 95:e1–e7.
22. Haddock, P. S., W. A. Coetzee, E. Cho, L. Porter, H. Katoh, D. M. Bers, M. S. Jafri, and M. Artman. 1999. Subcellular $[Ca^{2+}]i$ gradients during excitation-contraction coupling in newborn rabbit ventricular myocytes. *Circ. Res.* 85:415–427.
23. Yang, Z., C. Pascarel, D. S. Steele, K. Komukai, F. Brette, and C. H. Orchard. 2002. Na^{+}-Ca^{2+} exchange activity is localized in the T-tubules of rat ventricular myocytes. *Circ. Res.* 91:315–322.
24. Hamill, O. P., A. Marty, E. Neher, B. Sakmann, and F. J. Sigworth. 1981. Improved patch-clamp techniques for high-resolution current recording from cells and cell-free membrane patches. *Pflugers Arch.* 391:85–100.
25. Despa, S., F. Brette, C. H. Orchard, and D. M. Bers. 2003. Na/Ca exchange and Na/K-ATPase function are equally concentrated in transverse tubules of rat ventricular myocytes. *Biophys. J.* 85:3388–3396.
26. Mitchell, M. R., T. Powell, D. A. Terrar, and V. W. Twist. 1984. Strontium, nifedipine and 4-aminopyridine modify the time course of the action potential in cells from rat ventricular muscle. *Br. J. Pharmacol.* 81:551–556.
27. Brette, F., J. Leroy, J. Y. Le Guennec, and L. Salle. 2005. Ca^{2+} current in cardiac myocytes: old story, new insights. *Prog. Biophys. Mol. Biol.* DOI:10.1016/j.pbiomolbio.2005.01.001.
28. Fabiato, A. 1983. Calcium-induced release of calcium from the cardiac sarcoplasmic reticulum. *Am. J. Physiol.* 245:C1–14.

29. Page, E., and M. Surdyk-Droske. 1979. Distribution, surface density, and membrane area of diadic junctional contacts between plasma membrane and terminal cisterns in mammalian ventricle. *Circ. Res.* 45:260–267.

30. Hille, B. 1992. Ionic Channels of Excitable Membranes, 2nd ed. Sinauer Associates, Sunderland, MA.

31. Bers, D. M. 2001. Excitation-Contraction Coupling and Cardiac Contractile Force, 2nd ed. Kluwer Academic, Dordrecht, The Netherlands.

32. McDonald, T. F., S. Pelzer, W. Trautwein, and D. J. Pelzer. 1994. Regulation and modulation of calcium channels in cardiac, skeletal, and smooth muscle cells. *Physiol. Rev.* 74:365–507.

33. Franzini-Armstrong, C., F. Protasi, and V. Ramesh. 1999. Shape, size, and distribution of Ca^{2+} release units and couplons in skeletal and cardiac muscles. *Biophys. J.* 77:1528–1539.

34. Komukai, K., F. Brette, T. T. Yamanushi, and C. H. Orchard. 2002. K^+ current distribution in rat sub-epicardial ventricular myocytes. *Pflugers Arch.* 444:532–538.

35. Brette, F., P. Rodriguez, K. Komukai, J. Colyer, and C. H. Orchard. 2004. Beta-adrenergic stimulation restores the Ca transient of ventricular myocytes lacking t-tubules. *J. Mol. Cell. Cardiol.* 36: 265–275.

36. Bers, D. M., W. H. Barry, and S. Despa. 2003. Intracellular Na^+ regulation in cardiac myocytes. *Cardiovasc. Res.* 57:897–912.

37. Sah, R., R. J. Ramirez, and P. H. Backx. 2002. Modulation of Ca^{2+} release in cardiac myocytes by changes in repolarization rate: role of phase-1 action potential repolarization in excitation-contraction coupling. *Circ. Res.* 90:165–173.

38. Sah, R., R. J. Ramirez, G. Y. Oudit, D. Gidrewicz, M. G. Trivieri, C. Zobel, and P. H. Backx. 2003. Regulation of cardiac excitation-contraction coupling by action potential repolarization: role of the transient outward potassium current (I(to)). *J. Physiol.* 546:5–18.

39. Yuan, W., K. S. Ginsburg, and D. M. Bers. 1996. Comparison of sarcolemmal calcium channel current in rabbit and rat ventricular myocytes. *J. Physiol.* 493:733–746.

40. Takamatsu, H., T. Nagao, H. Ichijo, and S. Adachi-Akahane. 2003. L-type Ca^{2+} channels serve as a sensor of the SR Ca^{2+} for tuning the efficacy of Ca^{2+}-induced Ca^{2+} release in rat ventricular myocytes. *J. Physiol.* 552:415–424.

41. Terracciano, C. M., and K. T. MacLeod. 1997. Measurements of Ca^{2+} entry and sarcoplasmic reticulum Ca^{2+} content during the cardiac cycle in guinea pig and rat ventricular myocytes. *Biophys. J.* 72:1319–1326.

42. Puglisi, J. L., W. Yuan, J. W. Bassani, and D. M. Bers. 1999. Ca^{2+} influx through Ca^{2+} channels in rabbit ventricular myocytes during action potential clamp: influence of temperature. *Circ. Res.* 85:e7–e16.

43. Janczewski, A. M., and E. G. Lakatta. 1993. Buffering of calcium influx by sarcoplasmic reticulum during the action potential in guinea-pig ventricular myocytes. *J. Physiol.* 471:343–363.

44. Guia, A., M. D. Stern, E. G. Lakatta, and I. R. Josephson. 2001. Ion concentration-dependence of rat cardiac unitary L-type calcium channel conductance. *Biophys. J.* 80:2742–2750.

45. Inoue, M., and J. H. Bridge. 2003. Ca^{2+} sparks in rabbit ventricular myocytes evoked by action potentials: involvement of clusters of L-type Ca^{2+} channels. *Circ. Res.* 92:532–538.

46. Josephson, I. R., A. Guia, E. G. Lakatta, and M. D. Stern. 2002. Modulation of the gating of unitary cardiac L-type Ca^{2+} channels by conditioning voltage and divalent ions. *Biophys. J.* 83:2575–2586.

47. Lew, W. Y., L. V. Hryshko, and D. M. Bers. 1991. Dihydropyridine receptors are primarily functional L-type calcium channels in rabbit ventricular myocytes. *Circ. Res.* 69:1139–1145.

48. Rose, W. C., C. W. Balke, W. G. Wier, and E. Marban. 1992. Macroscopic and unitary properties of physiological ion flux through L-type Ca^{2+} channels in guinea-pig heart cells. *J. Physiol.* 456:267–284.

49. Soeller, C., and M. B. Cannell. 1997. Numerical simulation of local calcium movements during L-type calcium channel gating in the cardiac diad. *Biophys. J.* 73:97–111.

50. Stern, M. D., L. S. Song, H. Cheng, J. S. Sham, H. T. Yang, K. R. Boheler, and E. Rios. 1999. Local control models of cardiac excitation-contraction coupling. A possible role for allosteric interactions between ryanodine receptors. *J. Gen. Physiol.* 113:469–489.

51. Brochet, D. X., D. Yang, A. Di Maio, W. J. Lederer, C. Franzini-Armstrong, and H. Cheng. 2005. Ca^{2+} blinks: rapid nanoscopic store calcium signaling. *Proc. Natl. Acad. Sci. USA.* 102:3099–3104.

52. Shannon, T. R., T. Guo, and D. M. Bers. 2003. Ca^{2+} scraps: local depletions of free $[Ca^{2+}]$ in cardiac sarcoplasmic reticulum during contractions leave substantial Ca^{2+} reserve. *Circ. Res.* 93:40–45.

53. Balijepalli, R. C., A. J. Lokuta, N. A. Maertz, J. M. Buck, R. A. Haworth, H. H. Valdivia, and T. J. Kamp. 2003. Depletion of T-tubules and specific subcellular changes in sarcolemmal proteins in tachycardia-induced heart failure. *Cardiovasc. Res.* 59:67–77.

54. He, J., M. W. Conklin, J. D. Foell, M. R. Wolff, R. A. Haworth, R. Coronado, and T. J. Kamp. 2001. Reduction in density of transverse tubules and L-type Ca^{2+} channels in canine tachycardia-induced heart failure. *Cardiovasc. Res.* 49:298–307.

55. Quinn, F. R., S. Currie, A. M. Duncan, S. Miller, R. Sayeed, S. M. Cobbe, and G. L. Smith. 2003. Myocardial infarction causes increased expression but decreased activity of the myocardial Na^+-Ca^{2+} exchanger in the rabbit. *J. Physiol.* 553:229–242.